SHOEMAKER, D. P., ROBSON, M. E. & BROUSSARD, L. (1973). *Molecular Sieves*, edited by J. B. VYTTERHOVEN, p. 138. Leuven Univ. Press.
SMITH, J. V. (1978). *Am. Mineral.* **63**, 960–969.
SMITH, J. V. (1979). *Am. Mineral.* **64**, 551–562.
VON DREELE, R. B., JORGENSEN, J. D. & WINDSOR, C. G. (1982). *J. Appl. Cryst.* **15**, 581–589.
WILSON, S. T., LOK, B. M. & FLANIGEN, E. M. (1982). US Patent 4 310 440.
WILSON, S. T., LOK, B. M., MESSINA, C. A., CANNAN, T. R. & FLANIGEN, E. M. (1982). *J. Am. Chem. Soc.* **104**, 1146–1167.
WILSON, S. T., LOK, B. M., MESSINA, C. A., CANNAN, T. R. & FLANIGEN, E. M. (1983). *Am. Chem. Soc. Symp. Ser.* **218**, 79–106.

Acta Cryst. (1988). B**44**, 373–377

Structure of Sapphirine: its Relation to the Spinel, Clinopyroxene and β-Gallia Structures

BY J. BARBIER

Department of Chemistry, McMaster University, Hamilton, Ontario L8S 4M1, Canada

AND B. G. HYDE

Research School of Chemistry, Australian National University, GPO Box 4, Canberra, ACT 2601, Australia

(*Received* 23 *December* 1987; *accepted* 24 *March* 1988)

Abstract

A new description of the sapphirine structure is proposed in which it is shown to result from the regular intergrowth at the unit-cell level of slabs of the spinel and clinopyroxene structures. The latter structure is also shown to be simply related to the β-gallia structure by a periodic slip operation. These two structural relations appear to be directly relevant to the complex crystal chemistry of sapphirine.

1. Introduction

Sapphirine with the ideal composition $Mg_4Al_8Si_2O_{20}$ is an uncommon mineral, the crystal structure of which remained unsolved for a long time. Moore (1968, 1969) carried out the first structure determination for the monoclinic form (sapphirine-2M) while, more recently, Merlino (1980) determined the structure of the triclinic form (sapphirine-1Tc). Both polymorphs have cubic close-packed O atoms and their X-ray diffraction spectra show strong similarities to that of spinel, but no simple relationship could be established between the sapphirine and spinel structures. For instance, Moore (1969) referred to the topology of sapphirine as being 'quite distinct' from that of spinel.

The recent identification of a new sapphirine-like phase, $Mg_4Ga_8Ge_2O_{20}$ (Barbier, 1988), led us to re-examine this structure type in terms of its possible relationship to spinel.* This resulted in a new description of the sapphirine structure which is presented here and which is based on the intergrowth at the unit-cell level of spinel/β-gallia or spinel/pyroxene structural elements.

2. The sapphirine structure

Chemical analyses of natural and synthetic sapphirines commonly yield compositions slightly enriched in aluminium *via* the substitution reaction $2Al = Mg + Si$ (*e.g.* Higgins, Ribbe & Herd, 1979; Bishop & Newton, 1975). Nevertheless, the ideal stoichiometry $Mg_4Al_8Si_2O_{20}$ will be used here for simplicity and also because it directly results from the building principle of the sapphirine structure (see below).

The structure of sapphirine-2M [$P2_1/a$, $a = 11{\cdot}266$, $b = 14{\cdot}401$, $c = 9{\cdot}929$ Å, $\beta = 125{\cdot}46°$, $Z = 4$ (Moore, 1969)] is shown in Fig. 1 projected along the **a*** direction. It is based on an approximate cubic close packing of O atoms with (Mg, Al) and (Al, Si) atoms in octahedral and tetrahedral coordination, respectively. Owing to the difficulty of visualizing the sapphirine structure as a whole (*i.e.*, there is no short projection axis), its description by Moore (1969) and Merlino (1980) merely emphasized various structural elements within the {100} planes, such as walls of edge-sharing octahedra running parallel to **c**, separated by 'winged' pyroxene-like tetrahedral chains in the **b** direction and by isolated octahedra in the **a** direction.

Previous studies of sapphirine polymorphism (Merlino, 1973, 1980; Dornberger-Schiff & Merlino, 1974) also recognized that the structures of the monoclinic and triclinic forms are the end members of an order–disorder series corresponding to different stacking sequences of equivalent {010} layers. The width of

* Two other spinel-related compounds, $Mg_3Ga_2GeO_8$ (Barbier & Hyde, 1986) and $Mg_7Ga_2GeO_{12}$ (Barbier & Hyde, 1987), have previously been identified in the MgO–Ga_2O_3–GeO_2 system.

0108-7681/88/040373-05$03.00

one layer is $b_0 = 7{\cdot}2$ Å and the structure of sapphirine-2M (with $b = 14{\cdot}40$ Å) corresponds to a two-layer stacking (*cf.* Fig. 1), adjacent layers being related by the translation vectors $t_1 = a/2 + b_0 - c/4$ and $t_2 = a/2 + b_0 + c/4$ in the sequence $t_1\, t_2\, t_1\, t_2 \ldots$.* The single-layer stacking $t_1\, t_1\, t_1$ (or, equivalently, $t_2\, t_2\, t_2$) leads to the triclinic structure of sapphirine-1Tc which is, in all other aspects, very similar to that of sapphirine-2M (Merlino, 1980). For that reason, the present description of structural relations will be restricted to the latter but is also similarly applicable to the former.

3. Relation to the spinel and β-gallia structures

The spinel structure (idealized to perfect cubic close packing of anions) is shown in Fig. 2 projected along the [111] direction. As described by Hyde, White, O'Keeffe & Johnson (1982), it is built of identical one-octahedron-wide $\{\bar{1}10\}$ slabs with the AB_2O_4 stoichiometry, adjacent slabs being related by antiphase boundaries (S) with a displacement vector $\mathbf{R} = \mathbf{a}[112]/4$.†

* Note also that adjacent layers are related by the 2_1 axis parallel to **b** while individual layers are their own image in the **a**-glide reflection planes parallel to (010).

† The antiphase nature of the S boundaries is best seen in the [110] projection of the spinel structure as shown in Fig. 1 of Hyde *et al.* (1982).

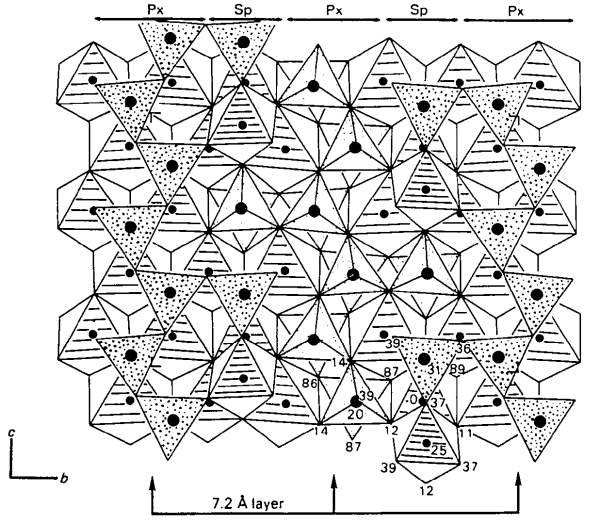

Fig. 1. The structure of monoclinic sapphirine-2M viewed along the **a*** direction. Only one half of the unit cell is drawn corresponding to $-0{\cdot}15 < x < 0{\cdot}50$ (the upper half is identical and related to the lower half by the **a**-glide planes at $y = \pm\frac{1}{4}$). The structure is based on an approximate cubic close packing of O atoms with octahedral (Mg, Al) and tetrahedral (Al, Si) atoms and is built from an ordered intergrowth of spinel (Sp) and pyroxene (Px) (010) slabs. The 7·2 Å layers common to sapphirine-2M and sapphirine-1Tc have been indicated. The structure of the triclinic polymorph can similarly be described in terms of a spinel + pyroxene intergrowth [*cf.* Figs. 1 and 2 in Merlino (1980)].

The relationship existing between the sapphirine and spinel structures becomes obvious when comparing Figs. 1 and 2 and examining the structural arrangement within the 7·2 Å $\{010\}$ layers of the sapphirine structure: the central portion of these layers (about one octahedron in width and noted Sp in Fig. 1) is identical to the $\{\bar{1}10\}$ slabs in spinel. Half of the remaining tetrahedra are also in the spinel configuration while the other half form corner-sharing tetrahedral pairs which, together with the remaining octahedra, give a local arrangement identical to that found in the β-gallia structure (Geller, 1960; *cf.* Fig. 3). It follows that the structure of individual 7·2 Å layers in sapphirine (and therefore the sapphirine structure as a whole) consists of an intergrowth of spinel and β-gallia structural elements. The stacking of these layers leads to the formation of chains of corner-sharing tetrahedra at the interlayer boundaries which are shown below to correspond to a pyroxene-like structure.*

The presence of spinel slabs within the sapphirine structure is reflected in the following simple geometrical relationships between their unit cells (for sapphirine-2M):

$$\mathbf{a}_{\text{sapph}} = \mathbf{a}_{\text{Sp}}[110]$$
$$\mathbf{c}_{\text{sapph}} = 1/2\mathbf{a}_{\text{Sp}}\,[\bar{1}\bar{1}2]$$
$$\beta_{\text{sapph}} = [110], [\bar{1}\bar{1}2].$$

$\mathbf{b}_{\text{sapph}}$ is parallel to the $[\bar{1}10]_{\text{Sp}}$ direction and its length, 14·40 Å, is equal to 5 × 2·88 Å which is a typical value for the octahedral (or tetrahedral) edge length in an oxygen close-packed array.

* Although the layer-stacking sequences are different in monoclinic and triclinic sapphirine, they both lead to structurally equivalent interlayer boundaries [*cf.* Figs. 1 and 2 in Merlino (1980)].

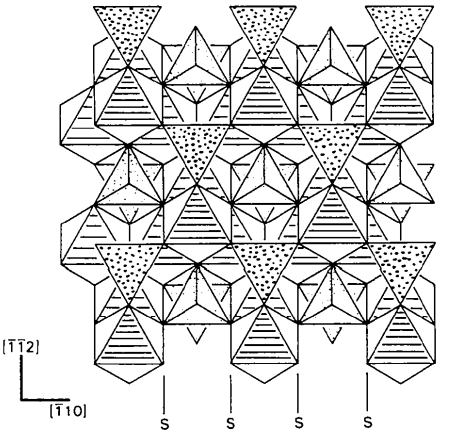

Fig. 2. The spinel structure (idealized to perfect cubic close-packed anion array) viewed along the [111] direction. The structure is built of identical one-octahedron-wide $\{\bar{1}10\}$ slabs related by antiphase boundaries (S). The same slabs are also present in the sapphirine structure (*cf.* Fig. 1).

4. Relation to the clinopyroxene structure

The structure of the low-temperature clinopyroxene form of $MgGeO_3$ [$C2/c$, $a = 9{\cdot}605$, $b = 8{\cdot}8940$, $c = 5{\cdot}160$ Å, $\beta = 100{\cdot}95°$, $Z = 8$ (Yamanaka, Hirano & Takeuchi, 1985)] is shown in Fig. 4 projected along the **a*** direction. Unlike the silicate pyroxenes, $MgGeO_3$ is based on a rather regular cubic close packing of O atoms which also occurs in $CoGeO_3$ (Peacor, 1968). The structure contains characteristic zigzag double chains of corner-sharing GeO_4 tetrahedra running parallel to **c**, adjacent chains being indirectly linked *via* corner sharing with walls of edge-sharing MgO_6 octahedra.

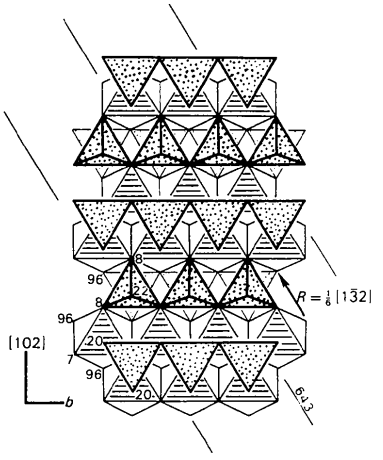

Fig. 3. The β-gallia structure viewed along the [10$\bar{2}$] direction. Only part of the structure is drawn corresponding to $-17 <$ heights $<$ 22 (heights given in 1/100 of the repeat distance in the projection direction). The structure is based on an approximate c.c.p. oxygen array with Ga atoms in both octahedral and tetrahedral coordination. It contains characteristic linear [010] double chains of corner-sharing GaO_4 tetrahedra. Note that β-gallia structural elements are also present in the sapphirine structure (*cf.* Fig. 1). The slip operation transforming the β-gallia structure into the clinopyroxene structure is indicated in the figure {displacement vector $R = \frac{1}{6}$[1$\bar{3}$2] on (643) planes}. Note that the [102], [1$\bar{3}$2] and (643) indices in the figure refer to an undistorted c.c.p. oxygen array.

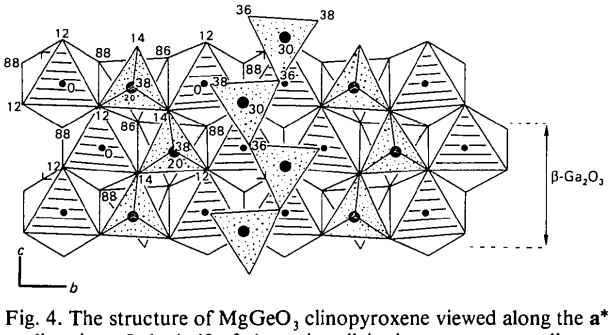

Fig. 4. The structure of $MgGeO_3$ clinopyroxene viewed along the **a*** direction. Only half of the unit cell is drawn corresponding to $-0{\cdot}15 < x < 0{\cdot}50$ (the upper half is identical and related to the lower half by the C-centering operation). The structure is based on an approximate cubic close packing of O atoms with octahedral (Mg) and tetrahedral (Ge) cations. It contains characteristic zigzag double chains of corner-sharing GeO_4 tetrahedra running parallel to the **c** direction which are also found in the sapphirine structure (*cf.* Fig. 1). The clinopyroxene structure can also be described as a stacking of β-gallia slabs in the **c** direction (one slab is indicated in the figure), adjacent slabs being related by a slip operation with a displacement vector of $\pm$**b**/3.

The relationship between the sapphirine and clinopyroxene structures is readily apparent by comparing Figs. 1 and 4: the spinel slabs (Sp) in the sapphirine structure alternate along the **b** direction with pyroxene slabs (Px). The latter are about one-and-a-half octahedra wide and are centered on the boundaries between adjacent 7·2 Å layers. They contain the double tetrahedral chains (without the wings) plus part of the octahedral walls above and below the chains and part of the adjacent octahedra at half height between the chains.

5. Relation between the β-gallia and clinopyroxene structures

Examination of the equivalent projections of the $MgGeO_3$ and β-Ga_2O_3 structures (down **a*** and [10$\bar{2}$] in Figs. 4 and 3 respectively) reveals the existence of a simple slip relation between them. It is clear from Fig. 4 that the pyroxene structure is built from β-gallia slabs (two octahedra wide, perpendicular to **c**), adjacent slabs being shifted by a displacement vector $\pm$**b**/3 which, to a first approximation, leaves the oxygen array invariant ($b/3 = 2{\cdot}98$ Å, *i.e.*, the displacement corresponds to one octahedral or tetrahedral edge length in the c.c.p. oxygen array).

Alternatively, as shown in Fig. 3, the transformation of the β-gallia structure into the clinopyroxene structure is achieved by the insertion, in the former, of periodic out-of-phase boundaries parallel to (643) with a displacement vector equal to 1/6 [1$\bar{3}$2].

6. Some aspects of the crystal chemistry of sapphirine

The structural relations described above show that sapphirine can be described as a regular intergrowth at the unit-cell level of the spinel and clinopyroxene structures. Using its ideal stoichiometry, sapphirine can then be formally written as: $Mg_4Al_8Si_2O_{20} = 2MgAl_2O_4$ (Sp) + $2MgAl_2SiO_6$ (Px). However, cation distributions determined in natural sapphirines (Moore, 1969; Higgins & Ribbe, 1979; Merlino, 1980) all indicate that the spinel slabs are enriched in aluminium relative to the $MgAl_2O_4$ composition (with $MgO:Al_2O_3$ ratios around 1:2·5† and that the cation arrangement within these slabs corresponds to an

† As also occurs in the so-called 'non-stoichiometric' spinel phases formed at high temperature in systems such as MgO–Al_2O_3, NiO–Al_2O_3, MgO–Ga_2O_3, *etc.*

inverse spinel structure [with Al atoms occupying the $T(5)$ and $T(6)$ tetrahedral sites] while $MgAl_2O_4$ spinel itself has a predominantly normal structure [with tetrahedral Mg atoms (Hill, Craig & Gibbs, 1979)]. [It should be noted, however, that cation disordering takes place in $MgAl_2O_4$ at temperatures as low as 933 K (Yamanaka & Takeuchi, 1983)]. It may be suggested that this redistribution of Al atoms takes place within the sapphirine unit cell because of the limited 'solubility' of Al_2O_3 in $MgSiO_3$ enstatite [about 15 mol% *via* the exchange reaction $2Al = Mg + Si$ (Taylor, 1973)] which does not include the $MgAl_2SiO_6$ composition (*cf.* Fig. 5). Interestingly, the sapphirine cell dimensions can to some extent be correlated with the high Al content of the spinel slabs *via* the geometrical relationships given earlier (see §3): $1/\sqrt{2}a_{sapph} = 7{\cdot}97$ Å, a value which is very close to the parameter $a = 7{\cdot}98$ Å reported by Saalfeld & Jagodzinski (1957) for an alumina-rich spinel with the composition $MgO : 2{\cdot}5Al_2O_3$ (*i.e.*, the same composition as the spinel slabs in sapphirine); c_{sapph} corresponds to a larger parameter ($2/\sqrt{6}c_{sapph} = 8{\cdot}11$ Å) which can be interpreted as the expansion of the spinel slabs required to match the c dimension of the pyroxene slabs. (Notice in Fig. 1 how the tetrahedral chains are slightly expanded in the **c** direction as compared to an ideal c.c.p. oxygen array, presumably because of strong interactions between the tetrahedral cations.)

In the case of the $MgO–Ga_2O_3–GeO_2$ system, the simple structural relation existing between clino-$MgGeO_3$ and β-gallia (see §5) might allow a higher degree of atomic substitution (*via* the reaction $2Ga = Mg + Ge$), thus approaching (and perhaps including) the $MgGa_2GeO_6$ clinopyroxene composition. A systematic study of the $MgGeO_3–Ga_2O_3$ join will be undertaken in order to elucidate this point. It is also noteworthy that $MgGa_2O_4$ spinel adopts an inverse structure (Hill *et al.*, 1979) like that expected for the spinel slabs in $Mg_4Ga_8Ge_2O_{20}$ sapphirine. It therefore appears that the gallogermanate system would be more favourable for the formation of a sapphirine phase than the aluminosilicate system. (Indeed, the uncommon natural occurrence of $Mg_4Al_8Si_2O_{20}$ sapphirine indicates that its formation requires rather specific conditions.)

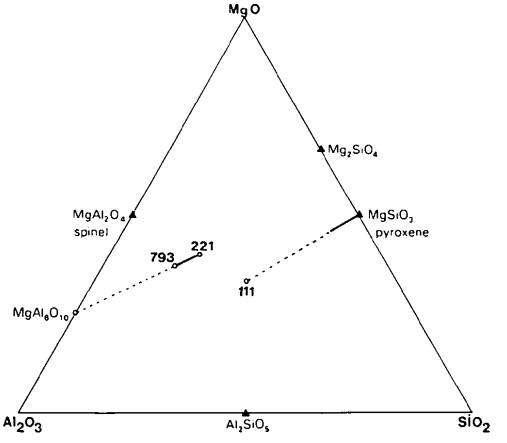

Fig. 5. Schematic phase diagram of the $MgO–Al_2O_3–SiO_2$ system showing the composition ranges of the sapphirine and pyroxene structures associated with the exchange reaction $2Al = Mg + Si$. All compositions are given as $MgO : Al_2O_3 : SiO_2$ molar ratios. $MgAl_6O_{10}$ corresponds to the composition of the hypothetical Si-free sapphirine.

The range of chemical compositions observed in natural sapphirines is indicated in Fig. 5: it varies between the 4 : 4 : 2 and 7 : 9 : 3 compositions (expressed in terms of $MgO : Al_2O_3 : SiO_2$ molar ratios) and is associated with the exchange reaction $2Al = Mg + Si$ (Higgins, Ribbe & Herd, 1979). In view of the present description of sapphirine as a spinel + pyroxene intergrowth, it may be argued that this limited $Al/(Mg + Si)$ substitution takes place primarily within the pyroxene part of the structure (*cf.* the solubility of Al_2O_3 in $MgSiO_3$ mentioned above). Complete substitution would lead to a silicon-free sapphirine with the $MgAl_6O_{10}$ composition (or a germanium-free $MgGa_6O_{10}$ sapphirine in the $MgO–Ga_2O_3–GeO_2$ system). As noted earlier by Moore (1969), the composition of these hypothetical sapphirines corresponds to that reported for some metastable phases in, for instance, the $MgO–Al_2O_3$ and $MgO–Ga_2O_3$ systems (*cf.* Bassoul, Lefebvre & Gilles, 1974) suggesting that they may be structurally related. The present study would suggest further that these metastable aluminate and gallate phases are based on a building principle similar to that of sapphirine and result from the intergrowth of spinel slabs (of the type found in sapphirine, see Fig. 1) with elements of the β-gallia structure [since complete $Ga/(Mg + Ge)$ substitution would promote transformation of the pyroxene slabs].

Finally, the building principle of both the 2M and 1Tc sapphirine unit cells from spinel and pyroxene (010) slabs naturally leads to the possibility of microstructural stacking disorder and intergrowths as reported by Merlino (1980). Indeed, during the completion of this work, we were made aware of an investigation of the defect structure of natural and synthetic sapphirines by high-resolution electron microscopy (Christy & Putnis, 1988) reporting the observation of new polytypes and (010) planar faults corresponding to the elimination of one spinel slab from the sapphirine unit cell. Stacking disorder has also been observed in synthetic sapphirines in the $MgO–Ga_2O_3–GeO_2$ system and is presently being investigated by electron diffraction/microscopy (Barbier, 1988).

References

BARBIER, J. (1988). In preparation.

BARBIER, J. & HYDE, B. G. (1986). *Phys. Chem. Miner.* **13**, 382–392.

BARBIER, J. & HYDE, B. G. (1987). *Acta Cryst.* B**43**, 34–40.

BASSOUL, P., LEFEBVRE, A. & GILLES, J. C. (1974). *J. Solid State Chem.* **10**, 56–65.
BISHOP, F. C. & NEWTON, R. C. (1975). *J. Geol.* **83**, 511–517.
CHRISTY, A. G. & PUTNIS, A. (1988). *Phys. Chem. Miner.* In the press.
DORNBERGER-SCHIFF, K. & MERLINO, S. (1974). *Acta Cryst.* A**30**, 168–173.
GELLER, S. (1960). *J. Chem. Phys.* **33**, 676–684.
HIGGINS, J. B. & RIBBE, P. H. (1979). *Contrib. Mineral. Petrol.* **68**, 357–368.
HIGGINS, J. B., RIBBE, P. H. & HERD, R. K. (1979). *Contrib. Mineral. Petrol.* **68**, 349–356.
HILL, R. J., CRAIG, J. R. & GIBBS, G. V. (1979). *Phys. Chem. Miner.* **4**, 317–339.
HYDE, B. G., WHITE, T. J., O'KEEFFE, M. & JOHNSON, A. W. S. (1982). *Z. Kristallogr.* **160**, 53–62.
MERLINO, S. (1973). *Contrib. Mineral. Petrol.* **41**, 23–29.
MERLINO, S. (1980). *Z. Kristallogr.* **151**, 91–100.
MOORE, P. B. (1968). *Nature (London)*, **218**, 81–82.
MOORE, P. B. (1969). *Am. Mineral.* **54**, 31–49.
PEACOR, D. R. (1968). *Z. Kristallogr.* **126**, 299–306.
SAALFELD, H. & JAGODZINSKI, H. (1957). *Z. Kristallogr.* **109**, 87–109.
TAYLOR, H. C. J. (1973). *Geol. Soc. Am. Bull.* **84**, 1335–1348.
YAMANAKA, T., HIRANO, M. & TAKEUCHI, Y. (1985). *Am. Mineral.* **70**, 365–374.
YAMANAKA, T. & TAKEUCHI, Y. (1983). *Z. Kristallogr.* **165**, 65–78.

Acta Cryst. (1988). B**44**, 377–380

Structures of Ce_2Sn_5 and Ce_3Sn_7, Two Superstructures of $CeSn_3$

BY J. X. BOUCHERLE

Département de Recherche Fondamentale/Service de Physique/MDN, Commissariat à l'Energie Atomique – Centre d'Etudes Nucleaires de Grenoble, 85X, 38041 Grenoble CEDEX, France

F. GIVORD

Laboratoire Louis Néel, Centre National de la Recherche Scientifique, 166X, 38042 Grenoble CEDEX, France

P. LEJAY

Centre de Recherche sur les Très Basses Températures, Centre National de la Recherche Scientifique, 166X, 38042 Grenoble CEDEX, France

AND J. SCHWEIZER AND A. STUNAULT

Département de Recherche Fondamentale/Service de Physique/MDN, Commissariat à l'Energie Atomique – Centre d'Etudes Nucleaires de Grenoble, 85X, 38041 Grenoble CEDEX, France

(*Received* 22 *April* 1987; *accepted* 17 *March* 1988)

Abstract

Ce_2Sn_5 and Ce_3Sn_7 crystallize in two new structures which are superstructures of cubic $CeSn_3$ ($AuCu_3$ type). They are orthorhombic with space group *Cmmm*. Their lattice parameters are related to that of $CeSn_3$ with $b(Ce_2Sn_5) \simeq 7a(CeSn_3)$ and $b(Ce_3Sn_7) \simeq 5a(CeSn_3)$. These superstructures are deduced from the cubic $CeSn_3$ structure by ordered atomic substitutions. In both cases these substitutions induce two crystallographic sites for the Ce atoms: one which has practically the same environment as that of Ce in $CeSn_3$, with only Sn atoms as first neighbours, and one with two Ce atoms among the first neighbours. Crystal data: Ce_2Sn_5, $a = 4{\cdot}559\ (6)$, $b = 35{\cdot}014\ (39)$, $c = 4{\cdot}619(4)$ Å, $R = 0{\cdot}048$ for 303 independent reflections; Ce_3Sn_7, $a = 4{\cdot}524(1)$, $b = 25{\cdot}742(11)$, $c = 4{\cdot}610\ (2)$ Å, $R = 0{\cdot}077$ for 191 independent reflections.

0108-7681/88/040377-04$03.00

Introduction

The intermetallic compound $CeSn_3$, which crystallizes in the cubic $AuCu_3$($L1_2$ type) structure, is considered to be a typical intermediate-valence compound. Therefore, the low-temperature magnetic susceptibility has been carefully studied by a large number of authors [see references given in Gschneidner, Dhar, Stierman, Tsang & McMasters (1985) and Boucherle, Fillion, Flouquet, Givord, Lejay & Schweizer (1986)] with particular attention to the increase of susceptibility at very low temperature ($T < 20$ K). Some of the authors consider this increase to be a result of the intermediate-valence character of cerium in this compound, but others attribute it to impurities and possibly to other phases of the Ce–Sn system.

To clarify this point, we have investigated the Ce–Sn compounds which can occur as impurities in $CeSn_3$. As the $AuCu_3$-type compounds may deviate from the $L1_2$